Proceedings of the 29th Annual International
Conference of the IEEE EMBS
Cité Internationale, Lyon, France
August 23-26, 2007.

Artificial Vitreous Humor for *In Vitro* Experiments

Michael P. Kummer, Jake J. Abbott, Sandro Dinser, and Bradley J. Nelson

Abstract— **In this paper we present a protocol to create artificial vitreous humor phantom tissue to be used as a test bed for *in vitro* experiments. The artificial vitreous consists of water, agar, and hyaluronic acid. Unlike existing vitreous replacement substances, this dummy tissue exhibits viscoelastic characteristics of *in vivo* natural vitreous humor. We are able to prepare artificial vitreous with a range of viscoelastic properties, which will allow us to account for the variation seen in human vitreous that comes with aging. The artificial vitreous will primarily serve as an experimental test bed for wireless magnetic control and vision-based tracking of assembled-MEMS microrobots. These microrobots will someday enable minimally invasive surgical and diagnostic intraocular procedures.**

I. INTRODUCTION

The vitreous humor is a viscoelastic, gel-like substance that fills the posterior cavity of the eye [1] as shown in Fig. 1. Since the early 1900's different materials have been used as vitreous replacements. As detailed in [2], these surrogates serve two main purposes. First, they are used to replace a dysfunctional vitreous humor in cases where opacification or the physical collapse and liquefaction of the vitreous has occurred. The second is their temporary or permanent application during retinal surgery. Since these substitutes are intended to be put in a patient's eye, they need to be transparent and, most importantly, biocompatible. In addition, the density and refractive index needs to be close to those of the natural vitreous. However, the viscoelastic properties of existing substitutes are not the same as those of the natural vitreous. Finding an optimal vitreous substitute is subject of ongoing research [3].

We are currently developing assembled-MEMS microrobots that are wirelessly controlled using externally applied magnetic fields. These untethered devices could navigate in bodily fluids to enable a number of new minimally invasive surgical and diagnostic procedures. We are particularly interested in ophthalmic procedures to address disorders such as retinal-vein occlusion. Ophthalmic procedures will require the microrobot to navigate through vitreous humor. Prior work by Yesin et al. [4] demonstrates that assembled-MEMS microrobots can be wirelessly controlled in a Newtonian-fluid environment. For precise control, we must characterize the behavior of assembled-MEMS microrobots being driven by external magnetic fields through vitreous humor, which is non-Newtonian.

This work is supported by the NCCR Co-Me of the Swiss National Science Foundation.

M. P. Kummer, J. J. Abbott, and B. J. Nelson are with the Institute of Robotics and Intelligent Systems, ETH Zurich, 8092 Zurich, Switzerland {kummerm, jabbott, bnelson}@ethz.ch

S. Dinser is with the Institute for Mechanical Systems, ETH Zurich, 8092 Zurich, Switzerland sandro.dinser@imes.mavt.ethz.ch

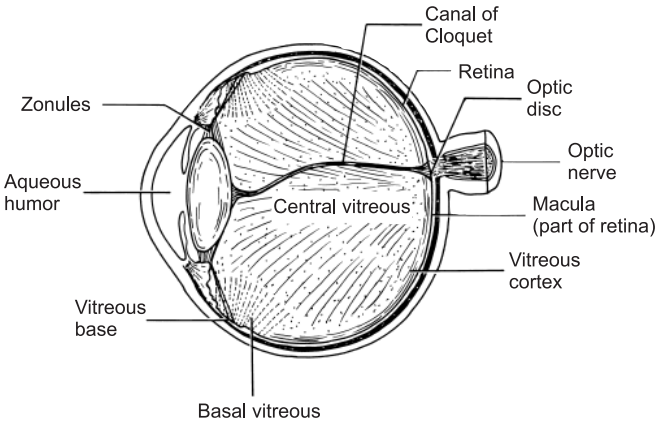

Fig. 1. Schematic cross section of an eye, reprinted from [7] with permission from Elsevier. The vitreous humor fills the posterior cavity of the eye.

In order to perform controlled experiments, we need a test bed that accurately represents the vitreous humor both mechanically and optically. We are not concerned with biocompatibility. Tissue-mimicking phantoms for controlled experiments in research related to the vitreous humor have been generated before [5]. Traditionally, these phantoms were generated using agar or acrylamide. However, they were applied for testing of acoustic measurement techniques and the focus was on the elastic properties of the eye. No existing phantom captures the viscoelastic nature of the vitreous.

An alternative is to use porcine or bovine cadaver eyes, but this alternative has several drawbacks. First, animal vitreous does not perfectly represent human vitreous. The eyes are not hygienic, they require appropriate storage, and they must be obtained from external sources. The properties of the vitreous change over the course of a human life due to liquefaction of the vitreous with increasing age [6]. Relative to humans, production animals die young, which leads to experimental test beds that represent a young population. Ophthalmic procedures, however, are mainly performed on the elderly.

To avoid these shortcomings and allow for an easy to prepare and inexpensive phantom vitreous, we have investigated a three-component mixture. In this paper we describe the protocol to create this vitreous-mimicking *in vitro* phantom tissue which exhibits properties of *in vivo* vitreous humor.

II. PREPARATION OF SAMPLES

The vitreous humor is made up of 99% water. The two other main components are collagen fibrils and hyaluronic acid. These two components serve a structural purpose [8],

[9]. The collagen fibrils run through the central vitreous in an antero-posterior way. Hyaluronic acid and water fill the spaces between the fibrils.

Although a hyaluronic acid solution is viscoelastic on its own, initial tests showed that the relative importance of the viscous and elastic components are reversed compared to those in natural vitreous humor. For this reason we chose agar (Ag), hyaluronic acid sodium salt (HA), and deionized water as the components for our mixture. The Ag (Fluka, CAS # 9002-18-0) comes in powder form and has a solubility of $15\,\mathrm{mg/ml}$ in water. It is used to add elasticity to the phantom tissue and mimic the properties of the collagen fibrils. While it does not have the ability to provide the structural properties of the actual collagen fibrils, it presents an inexpensive and simple way to add elasticity to the mixture. The HA (Fluka, CAS # 9067-32-7) is a granulate and has a solubility of $5\,\mathrm{mg/ml}$ in water. Since it is a component of the natural vitreous, it seemed to be an obvious component for a vitreous-mimicking phantom.

To prepare the samples, the desired amounts of Ag and HA where weighed and placed in a vial. Deionized water was brought to a boil and then rested until no bubbles were forming anymore. Then water was pipetted and added to the Ag and HA in the vials until the desired concentrations of Ag and HA were reached. Since the Ag needs to cook at $100\,^{\circ}\mathrm{C}$ for $15\,\mathrm{min}$ in order to dissolve properly, the vials were placed in a water quench immediately after mixing. Before placing the vials in the water quench, they were stirred vigorously. The samples were periodically stirred while they were sitting in the water quench. Upon removal of the samples from the water quench after $15\,\mathrm{min}$, the samples were stirred one last time before they were left to cool and gel for approximately $24\,\mathrm{h}$ at room temperature. After a period of $24\,\mathrm{h}$, the properties of the samples were measured.

To measure the viscoelastic properties of the different samples, a Physica UDS 200 rotational rheometer [10] was used in the cone/plate configuration. The room where the measurements were taken was climate controlled at $21\,^{\circ}\mathrm{C}$. In order to measure the viscoelastic properties of the samples, $7\,\mathrm{ml}$ of the sample gel needed to be loaded into the rheometer. In initial trials the samples where loaded using a $2\,\mathrm{ml}$ single-use syringe without a needle. However, these measurements proved to be inconsistent and showed poor reproducibility. Most likely the small opening of the syringe caused cleavage of the gel. Similar effects were observed in [11] when injecting hydrogels through small gauge needles into the eye. To avoid this problem, the loading syringe was modified by cutting off the distal end as shown in Fig. 2. This improved the reproducibility of the measurements significantly. Ideally, the sample would be prepared in the container that is used in the experiments.

III. RHEOMETRIC MEASUREMENTS AND REGRESSION ANALYSIS

The mechanical properties of viscoelastic fluids are typically measured using oscillatory shear force experiments [12]. Assuming a linear relation between shear stress and strain, when a viscoelastic fluid is subjected to an oscillating shear stress

Fig. 2. Syringe and modified syringe used to load rheometer.

$$\tau = \tau_0 \cos \omega t \tag{1}$$

the resulting shear strain will have the form

$$\gamma = \gamma_0 \cos\left(\omega t - \phi\right) \tag{2}$$

A phase lag $\phi = 0^{\circ}$ corresponds to a purely elastic material, and a phase lag $\phi = 90^{\circ}$ corresponds to a purely viscous material.

The complex shear modulus G^* is defined as the ratio of the shear stress to the shear strain:

$$G^* = G' + iG'' = \frac{\tau_0}{\gamma_0}\cos\phi + i\frac{\tau_0}{\gamma_0}\sin\phi \tag{3}$$

where G' is the storage modulus, which represents the elastic component of the fluid, and G'' is the loss modulus, which represents the viscous component. The storage and loss moduli are the values typically reported during rheometric measurements, and both are in units Pa. In the style of [13], oscillatory tests with constant frequency and variable strain were performed ($\omega = 10\,\mathrm{rad/s}$, $\gamma = 0.5 - 10\,\%$).

Samples with different concentrations of Ag and HA were measured. Nominal levels of 0.5, 1, 1.5, 2, and $3\,\mathrm{mg/ml}$ for [Ag] were paired with nominal levels of 0, 1, 2, 3, 3.5, 4, and $5\,\mathrm{mg/ml}$ for [HA]. The actual concentration values where within 1% of the nominal values. To enable statistical analysis on the measured data, each concentration pair was prepared three times. Each sample was measured twice over the entire strain range. A typical set of measurement curves for the series with $[Ag] = 3\,\mathrm{mg/ml}$ and $[HA] = 3\,\mathrm{mg/ml}$ is presented in Fig. 3. The figure shows that G' and G'' remain linear up to roughly 1.5% strain for this series. We found this to hold true for all samples. An average over the four lowest-strain values of each measurement was used to classify G' and G'' for the respective sample.

In Fig. 4 the measured G' values for the samples are shown. Every line represents a fixed HA concentration. The error bars represent the standard deviation between the three different samples for each concentration pair. The analogous plot for G'' is displayed in Fig. 5.

Using S-Plus, a regression analysis was performed on both the storage modulus and loss modulus data sets. For each of the storage and loss modulus, a function was assumed,

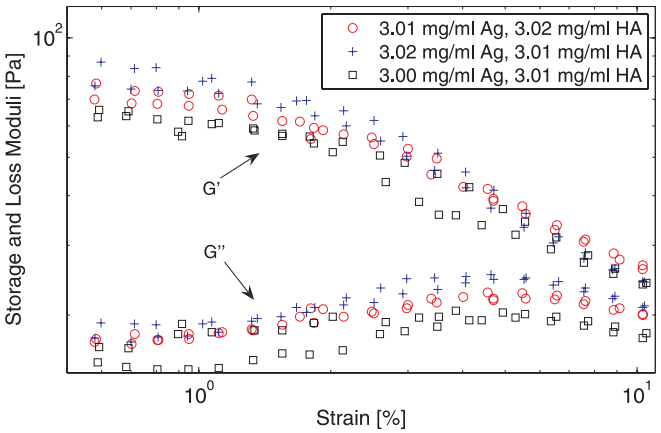

Fig. 3. Typical measurement result for a set of samples. In this case for the group with $[Ag] = 3\,\mathrm{mg/ml}$ and $[HA] = 3\,\mathrm{mg/ml}$.

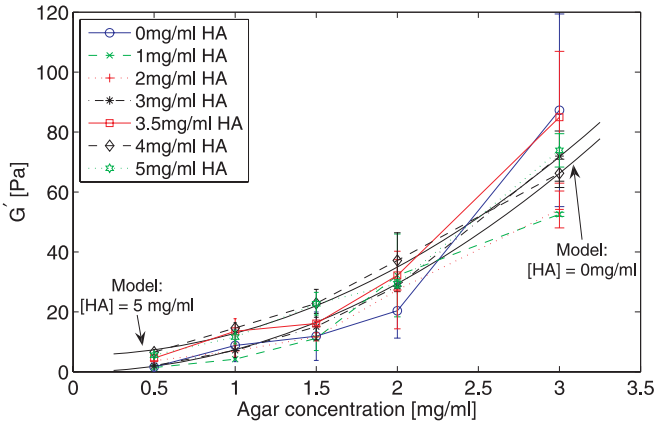

Fig. 4. Measured data for the storage modulus. Each line represents a fixed concentration of HA for varying concentrations of Ag. The error bars show the standard deviation between the three samples per point at a given mixture. The model is also shown for two concentrations.

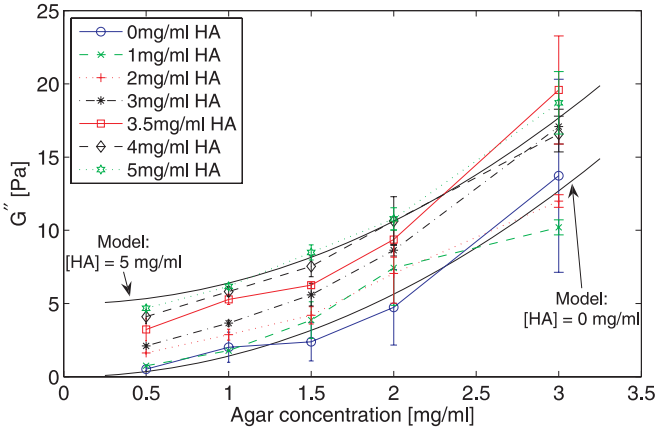

Fig. 5. Measured data for the loss modulus. Each line represents a fixed concentration of HA for varying concentrations of Ag. The error bars show the standard deviation between the three samples at a given mixture. The model is also shown for two concentrations.

where [Ag] and [HA] entered in linearly and quadratically. In addition to that an interaction term between [Ag] and [HA] was introduced. Assuming a 95% significance level, the regression led to the following equations for G' ($R^2 = 0.94$) and G'' ($R^2 = 0.96$):

$$G' = 7.36[Ag]^2 + 0.220[HA]^2 \quad (4)$$

$$G'' = 1.41[Ag]^2 + 0.997[HA] \quad (5)$$

Both equations assume [Ag] and [HA] in units $\mathrm{mg/ml}$, and G' and G'' in units Pa. Although Figs. 4 and 5 display the experimental data grouped by their nominal concentration values, the regression analysis utilized the actual values.

Comparing the equations with the respective data in Figs. 4 and 5 shows good agreement. In case of G' the quadratic relation between G' and [Ag] is apparent. We see that an addition of HA adds to G' yet in a less significant way than Ag, as evidenced by the coefficients. In the case of G'' again the quadratic relation between G'' and [Ag] is clear. In addition it can clearly be seen that the addition of HA raises the respective curve above a curve representing a smaller [HA]. We also observe a large variance in both the storage and loss moduli with high [Ag], and this variance is currently unexplained.

A second round of measurements was performed 48 h after creating the samples. However, the difference between the 24 h and 48 h measurements was negligible.

IV. PROTOCOL TO CREATE DESIRED VITREOUS

With (4) and (5) we are now equipped with the tools to generate our custom vitreous humor. All equations assume units as previously defined. Once the desired values for G' and G'' have been chosen, the first step is to solve (5) for $[Ag]$. This results in:

$$[Ag] = (0.709G'' - 0.707[HA])^{\frac{1}{2}} \quad (6)$$

The next step is to replace $[Ag]$ in (4) using (6). The result of this substitution yields the following quadratic equation for [HA]:

$$0 = 0.220[HA]^2 - 5.20[HA] + (5.22G'' - G') \quad (7)$$

The solution of this particular quadratic function with respect to [HA] is:

$$[HA]_{1,2} = \frac{5.20 \pm \sqrt{27.0 - 0.880\,(5.22G'' - G')}}{0.440} \quad (8)$$

In theory two values of [HA] can be calculated for desired values of G' and G''. Taking a closer look at the parameters in (8), however, reveals that only one of the two possible solutions yields a usable result. The solubility of HA as provided by the manufacturer is $5\,\mathrm{mg/ml}$ in water. This has not been verified by the authors. Knowing this limit induced by solubility, it has been found that only the result where the square-root term is subtracted yields a useable result. Once the required concentration of HA has been determined, the corresponding value for [Ag] can be calculated using (6).

There are limitations as to what values for G' and G'' can be realized. For one, if the term under the square-root in (8) is negative, the result will be a pair of imaginary numbers. So all value pairs

$$G' > 5.22G'' - 30.7 \quad (9)$$

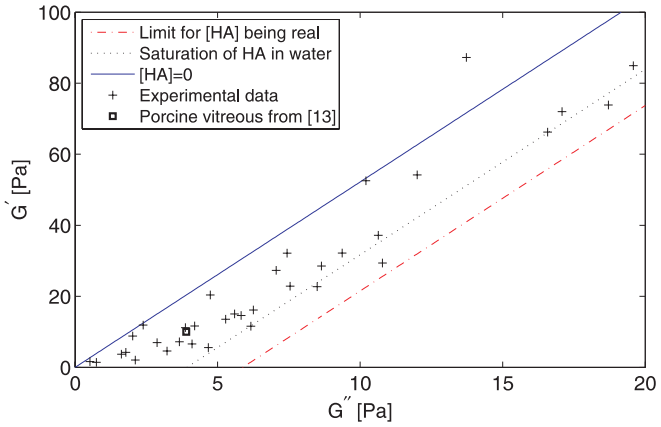

Fig. 6. Area of feasible storage and loss modulus pairs. The area between the solid and the dotted lines represents the attainable combinations of storage and loss moduli predicted by the model and limited by the reported saturation value of HA in water. The dash-dotted line represents the limit of (9), which creates no additional limitations on feasible pairs. Experimental data is shown for the mean values for each of the [Ag]-[HA] combinations. The values for porcine vitreous reported in [13] is also shown.

are out of range. The dash-dotted line in Fig. 6 represents (9). The solubility of HA also imposes a restriction on what value pairs of storage and loss moduli can be reached. Substituting $[HA] \leq 5\,\mathrm{mg/ml}$ in (8) and solving for G' we obtain:

$$G' \geq 5.22G'' - 20.5 \tag{10}$$

Thus before entering the domain of imaginary numbers from (9), the solubility of HA in water limits the modulus pairs to what is left of the dotted line in Fig. 6. Modulus pairs between the two broken lines in Fig. 6 require real number concentrations of HA, yet the values suggest a supersaturated HA solution. The solid line in Fig. 6 represents the limit when $[HA] = 0$, resulting in a second bounding condition:

$$G' \leq 5.22G'' \tag{11}$$

It can be observed in Figs. 4 and 5 that the variance in the measured data increases with increasing storage and loss moduli. It can also be observed in Fig. 6 that the boundaries predicted by the model are most accurate when the storage and loss moduli are relatively low.

As seen in Fig. 6, the values reported for porcine vitreous in [13] fall well within the achievable properties of the artificial vitreous. However, as reported in [13], there is some doubt over the true *in vivo* properties of the human vitreous. The viscoelastic properties of the vitreous change significantly within the first hour after removal from the dissected eye. In this time period, the material properties can change by a factor of five before appearing to reach a steady state. The result in [13] casts some doubt on the quantitative values previously reported for vitreous humor. However, it is likely that the artificial vitreous will be suitable for *in vitro* human models based on existing data [1], [13], [14].

V. CONCLUSIONS AND FUTURE WORKS

In this paper we have presented a protocol to generate an inexpensive phantom vitreous tissue that can be used for *in vitro* experiments. As opposed to animal cadaver eyes, a test bed with different properties can be generated depending on the desired vitreous viscoelastic properties. Furthermore, the samples proved to keep their properties over the course of at least two days without significant changes. This makes the samples suitable for tests that require a longer period of time.

In the future the optical properties of the three-component mixture will be measured. Visual inspection shows that the resulting mixtures are clear, yet only optical measurements will show whether the refractive index is close to that of real vitreous.

Kummer et al. [15] present a custom experimental system designed to measure the magnetic and hydrodynamic properties of the assembled-MEMS microrobots discussed in Section I. Thus far the hydrodynamic properties of the microrobots were measured only in Newtonian fluids. In the future we will measure the properties of the microrobots in the artificial vitreous humor presented here. Finally, the artificial vitreous will fill an artificial eye that will act as an experimental test bed for wireless magnetic control and vision-based tracking of intraocular microrobots.

REFERENCES

[1] T. V. Chirila and Y. Hong, "The vitreous humor," in *Handbook of Biomaterial Properties*, J. Black and G. Hastings, Eds. Chapman and Hall, 1998, pp. 125–131.

[2] T. V. Chirila, Y. Hong, P. D. Dalton, I. J. Constable, and M. F. Refojo, "The use of hydrophilic polymers as artificial vitreous," *Progress in Polymer Science*, vol. 23, pp. 475–508, 1998.

[3] N. Soman and R. Banerjee, "Artificial vitreous replacements," *Bio-Medical Materials and Engineering*, vol. 13, pp. 59–74, 2003.

[4] K. B. Yesin, K. Vollmers, and B. J. Nelson, "Modeling and control of untethered biomicrorobots in a fluidic environment using electromagnetic fields," *Int'l. J. Robotics Research*, vol. 25, no. 5–6, pp. 527–536, 2006.

[5] L. A. Negron, F. Viola, E. P. Black, C. A. Toth, and W. F. Walker, "Development and characterization of a vitreous mimicking material for radiation force imaging," *IEEE Trans. Ultrasonics, Ferroelectrics, and Frequency Control*, vol. 49, pp. 1543–1551, 2002.

[6] J. Sebag, "Age-related changes in human vitreous structure," *Graefe's Archive for Clinical and Experimental Ophthalmology*, vol. 225, no. 2, pp. 89–93, 1987.

[7] P. N. Bishop, "Structural macromolecules and supramolecular organisation of the vitreous gel," *Progress in Retinal and Eye Research*, vol. 19, pp. 323–344, 2000.

[8] H. Davson, *The Eye*, 2nd ed. 111 Fifth Avenue, New York, New York 10003: Academic Press, INC., 1969.

[9] J. Sebag and E. A. Balazs, "Morphology and ultrastructure of human vitreous fibers," *Investigative Ophthalmology & Visual Science*, vol. 30, no. 8, pp. 1867–1871, 1989.

[10] (2007) Anton Paar. [Online]. Available: http://www.anton-paar.com/

[11] T. V. Chirila and Y. Hong, "Poly(1-vinyl-2-pyrrolidinone) hydrogels as vitreous substitutes: a rheological study," *Polymer International*, vol. 46, pp. 183–195, 1997.

[12] R. B. Bird, R. C. Armstrong, and O. Hassager, *Dynamics of Polymeric Liquids*, 2nd ed. New York: John Wiley & Sons, 1987.

[13] C. S. Nickerson, "Engineering the mechanical properties of ocular tissues," Ph.D. dissertation, California Institute of Technology, 2005.

[14] B. Lee, M. Litt, and G. Buchsbaum, "Rheology of the vitreous body. Part I: Viscoelasticity of human vitreous," *Biorheology*, vol. 29, pp. 521–533, 1992.

[15] M. P. Kummer, J. J. Abbott, K. Vollmers, and B. J. Nelson, "Measuring the magnetic and hydrodynamic properties of assembled-MEMS microrobots," in *Proc. IEEE Int'l. Conf. Robotics and Automation*, 2007, pp. 1122–1127.